

PROCEEDINGS OF SPIE

[SPIEDigitallibrary.org/conference-proceedings-of-spie](https://www.spiedigitallibrary.org/conference-proceedings-of-spie)

Novel hyperspectral imaging approaches allow 3D measurement of cAMP signals in localized subcellular domains of human airway smooth muscle cells

Howard, Madison, Annamdevula, Naga, Pleshinger, D., Johnson, Santina, Beech, Luke, et al.

Madison Howard, Naga Annamdevula, D. J. Pleshinger, Santina Johnson, Luke Beech, Raymond B. Penn, C. Michael Francis, Thomas C. Rich, Silas J. Leavesley, "Novel hyperspectral imaging approaches allow 3D measurement of cAMP signals in localized subcellular domains of human airway smooth muscle cells," Proc. SPIE 11964, Imaging, Manipulation, and Analysis of Biomolecules, Cells, and Tissues XX, 119640I (3 March 2022); doi: 10.1117/12.2608267

SPIE.

Event: SPIE BiOS, 2022, San Francisco, California, United States

Novel Hyperspectral imaging approaches allow 3D measurement of cAMP signals in localized subcellular domains of human airway smooth muscle cells

Madison Howard¹, Naga Annamdevula^{2,3}, DJ Pleshinger^{2,3}, Santina Johnson^{2,3}, Luke Beech¹,
Raymond B. Penn⁴, C. Michael Francis⁵, Thomas C. Rich^{2,3}, and Silas J. Leavesley^{1,2,3}

¹Chemical and Biomolecular Engineering, University of South Alabama, Mobile, AL 36688

²Pharmacology, University of South Alabama, Mobile, AL 36688

³Center for Lung Biology, University of South Alabama, Mobile, AL 36688

⁴Medicine, Thomas Jefferson University, Philadelphia, PA 19107

⁵Physiology and Cell Biology, University of South Alabama, Mobile, AL 36688

ABSTRACT

Studies of the cAMP signaling pathway have led to the hypothesis that localized cAMP signals regulate distinct cellular responses. Much of this work focused on measurement of localized cAMP signals using cAMP sensors based upon Förster resonance energy transfer (FRET). FRET-based probes are comprised of a cAMP binding domain sandwiched between donor and acceptor fluorophores. Binding of cAMP triggers a conformational change which alters FRET efficiency. In order to study localized cAMP signals, investigators have targeted FRET probes to distinct subcellular domains. This approach allows detection of cAMP signals at distinct subcellular locations. However, these approaches do not measure localized cAMP signals per se, rather they measure cAMP signals at specific locations and typically averaged throughout the cell. To address these concerns, our group implemented hyperspectral imaging approaches for measuring highly multiplexed signals in cells and tissues. We have combined these approaches with custom analysis software implemented in MATLAB and Python. Images were filtered both spatially and temporally, prior to adaptive thresholding (OTSU) to detect cAMP signals. These approaches were used to interrogate the distributions of isoproterenol and prostaglandin-triggered cAMP signals in human airway smooth muscle cells (HASMCs). Results demonstrate that cAMP signals are spatially and temporally complex. We observed that isoproterenol- and prostaglandin-induced cAMP signals are triggered at the plasma membrane and in the cytosolic space. We are currently implementing analysis approaches to better quantify and visualize the complex distributions of cAMP signals. This work was supported by NIH P01HL066299, R01HL058506, and S10RR027535.

Key Words: spectroscopy, second messenger, microscopy, fluorescence, FRET, image cytometry, isoproterenol, PGE1

1. INTRODUCTION

As regulators of airway patency, human airway smooth muscle cells (HASMCs) are responsible for numerous airway functions in normal physiology and disease.¹ Abnormal HASMC function results in increased constriction of the airway and difficulty in breathing. Therefore, HASMCs are the primary therapeutic targets in obstructive airway diseases such as asthma and chronic obstructive pulmonary disorder (COPD). Beta agonists (β -agonists) are the drugs of choice for rescue from acute bronchoconstriction by activating β 2-adrenoceptors (β 2ARs) on airway smooth muscle, and mediating relaxation.^{2,3} The recognized cellular mechanism of action of β -agonists involves generation of cyclic AMP, and activation of its effector proteins, which antagonize smooth muscle contraction.⁴ Other agonists also increase cAMP levels and protein activity to modulate the contractile state of HASMCs. Despite the availability of such treatments, problems such as desensitization/tolerance, adverse side effects, or resistance prevent effective control of common symptoms associated with obstructive lung diseases. Hence, while cAMP plays a key role in HASMC contraction, it is not yet clear how different agonists encode for distinct physiological responses through the cAMP signaling pathway. Recent studies propose that the spatial distribution of cAMP signals is important to achieve signaling specificity.

FRET has been a standard approach for detecting cyclic nucleotide signals, such as cAMP. FRET reporters have allowed direct visualization of localized cAMP levels in living cells.⁵ When combined with spectral imaging, FRET reporters may be detected simultaneously with other molecular labels, while removing effects from autofluorescence and background signals.^{5,6} After imaging, the signals are typically quantified by selecting regions of interest corresponding to single cells or groups of cells. However, whole cell analysis of second messenger signals does not allow for quantification of the spatial distributions of those signals. Hence, a dynamic approach for quantifying the spatial characteristics of second messenger signals is needed.

Here we focus on illuminating the spatiotemporal signaling dynamics of cyclic AMP signals in HASMCs. To this end, we will employ hyperspectral FRET imaging methods to visualize agonist-induced spatial distributions of cAMP in HASMCs and we describe an automated image analysis approach that automatically identifies regions of interest for quantifying levels of cell second messenger signals. A region-based analysis approach called S8 was employed for analysis. To illustrate the potential for this approach, we have analyzed three dimensional and time lapse image data of cAMP signals in HASMCs. Preliminary results demonstrate that S8 allowed for automatic segmentation, which detected regions of varying cAMP levels and allowed tracking of changes in region size and shape over time. This approach will be especially helpful for understanding the relationship between spatially localized cell signaling and physiological outcomes, as well as objectively characterizing spatial and temporal properties of encoded signals.

2. METHODS

2.1 Cell Culture

HASMCs were cultured as previously described (Leavesley, 2021⁷). In brief, HASMCs were separated and placed in Dulbecco's Modified Eagles Medium. Cells were transferred to round coverslips at 37 °C and were grown to 70-80% confluence. Forty-eight hours prior to imaging, HASMCs were transfected with a H188 FRET sensor (Klarenbeek, 2015⁸). Cells were labeled with DRAQ5 (nuclear label) 10 minutes prior to imaging. The coverslip with adherent cells was placed in an attofluor cell chamber and bathed in 800 μL buffer. An additional 200 μL buffer, containing a sufficient concentration of isoproterenol or PGE₁ to bring the total concentration in the attofluor to either 1.0 μM or 0.1 μM, respectively.

2.2 Spectral imaging microscopy

Spectral imaging microscopy was performed as previously described (Annamdevula, 2018⁵). In summary, transfected cells were imaged using a Nikon A1R confocal microscope with 60x water immersion objective (Plan Apo VC 60x DIC N2 WI NA-1.2; Nikon Instruments, Melville, New York) and 32 channel spectral detector. Axial image stacks (z-stacks) were acquired every 30 seconds for a 20-minute period. An excitation wavelength of 405 nm (8% laser intensity = 1.82 μW at the sample stage) was used to excite the donor, Turquoise. Additionally, 561 nm (10% intensity = 19.02 μW at the sample stage) was used to excite the nuclear label, DRAQ5. Spectral emission was measured from 414 to 724 nm in 10 nm increments. One minute after baseline acquisition, HASMCs were treated with either isoproterenol or PGE₁.

2.3 Spectral image analysis

Spectral image analysis was performed as previously described (Annamdevula, 2018⁵). In summary, images were unmixed using a custom MATLAB script and smoothed using Gaussian filtering. FRET efficiency was calculated and mapped to cAMP concentration using the Hill Equation with a Hill coefficient of one. Agonist-induced changes in the subcellular distributions of cAMP concentrations were then investigated.

2.4 Region of interest-based feature analysis approach

Cyclic AMP spatial gradients were analyzed using a region-based analysis approach called S8, developed at the University of South Alabama. Analysis included both spatial and temporal smoothing of input images displaying cAMP concentrations as calculated from FRET image data. Intensity threshold values were calculated from smoothed images and were used to define one or more regions of interest within the image. Regions were then correlated between multiple time steps. Quantitative features, including region area, signal intensity, and others, were extracted from each region.

3. RESULTS AND DISCUSSION

The data presented in this paper are—three-dimensional, time lapse image data describing intracellular cAMP concentrations. From these data, spatial distributions of cAMP can be calculated and visualized as axial z-slices from the

apical to basal side of the cell. An overall goal of this research is to understand the nature of spatially- and temporally-dependent changes in cAMP concentrations and how these concentration profiles may affect downstream cellular physiology. To extract spatial and temporal features from the image data, we used an automated region-of-interest based analysis approach implemented in a custom software package (S8). The S8 software provides the capability to identifying regions of increased signal strength within an image using an automated intensity-based thresholding technique. These regions are individually segmented and assigned unique identifiers. Regions are tracked as they develop over time, including changes in location, size, and shape, as well as the relationship between regions that merge or divide over time.

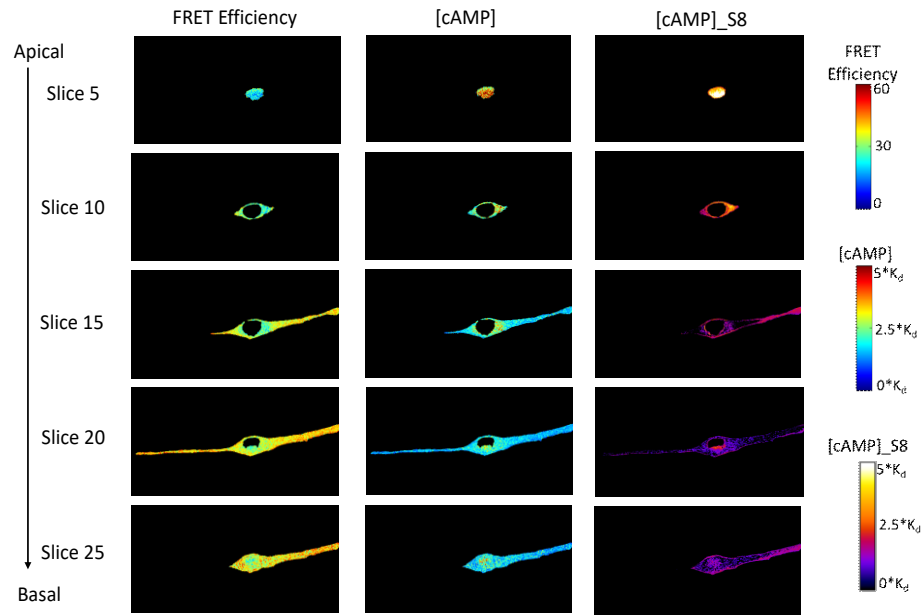


Figure 1: Visualization of isoproterenol-induced cAMP signals in a HASMC, 12 minutes after treatment with $0.1 \mu\text{M}$ isoproterenol, using spectral imaging and automated thresholding approaches. Cyclic AMP signals were monitored using the H188 FRET-based reporter. Three-dimensional data were acquired using a Nikon A1R confocal microscope. Five slices from the apical to the basal side of the cell are shown. In the left column, FRET efficiency data, determined from linearly unmixed Turquoise and Venus images, is displayed. The middle column shows cAMP concentrations calculated from FRET efficiency, assuming the binding behavior is governed by the Hill equation with a Hill coefficient equal to 1. The right column displays localized regions of cAMP concentrations that were determined using a region-of-interest based software called S8. It is important to note that S8 data processing includes both spatial and temporal smoothing that is statistically guided by the software.

As a proof-of-principle feasibility study, cAMP distributions in human airway smooth muscle cells were analyzed as a function of two treatment groups: $1.0 \mu\text{M}$ isoproterenol (Figure 1 and Figure 2) and $0.1 \mu\text{M}$ PGE₁ (Figure 3 and Figure 4). For the HASMCs treated with $1.0 \mu\text{M}$ isoproterenol, apical-to-basal cAMP spatial gradients can be seen to form with higher concentrations near the cell membrane at the apical side of the cell, and lower concentrations in the cytosol. These membrane-localized regions of cAMP were automatically identified in the S8 software (best visualized in Figure 1, slices 15 and 20). S8 software also identified paranuclear increases in cAMP concentration.

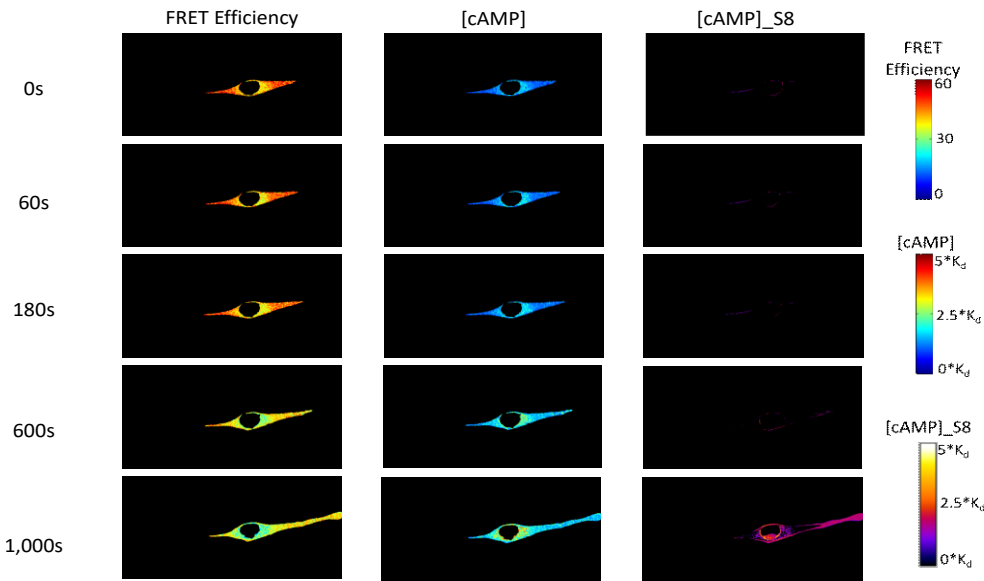


Figure 2: Visualization of time lapse isoproterenol-induced cAMP signals in a HASMC using spectral imaging and automated thresholding approaches. Cyclic AMP signals were monitored using the H188 FRET-based reporter. The cell was treated at 60s with $0.1 \mu\text{M}$ isoproterenol. Three-dimensional data were acquired using a Nikon A1R confocal microscope. Time points of z-slice 15, located midway through the cell, are shown. In the left column, FRET efficiency data, determined from linearly unmixed Turquoise and Venus images, is displayed. The middle column shows cAMP concentrations from FRET efficiency, assuming the binding behavior is governed by the Hill equation with a Hill coefficient equal to 1. The right column displays localized regions of cAMP concentrations that were determined using a region-of-interest based software called S8. It is important to note that S8 data processing includes both spatial and temporal smoothing that is statistically guided by the software.

When visualizing time lapse image data, localized regions of high cAMP concentration did not appear until time point 600 seconds (Figure 2). This change in cAMP was more at 1000 s. It is important to note that at the final time point, a high signal is detected, using S8, near the bottom portion of the image. This particular region may have appeared as a result of thresholding artifact of the DRAQ5 nuclear label. This artifact may have caused the S8 software to detect the change in area of the thresholded region as a large change in cAMP concentration in this region, therefore causing S8 to identify this as a region of interest.

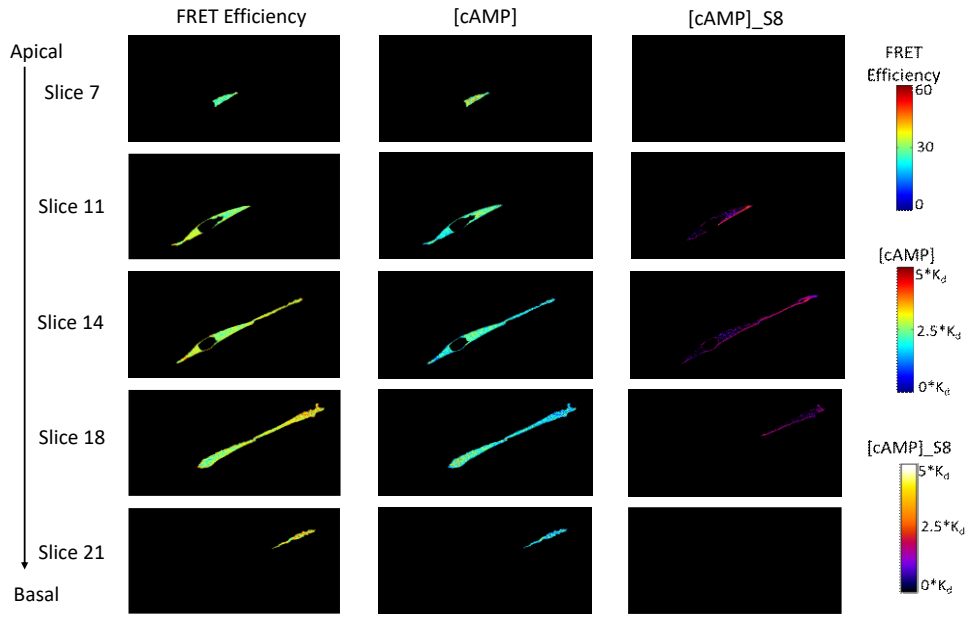


Figure 3: Visualization of PGE₁-induced cAMP signals in a HASMC, 12 minutes after treatment with 0.1 μ M PGE₁, using spectral imaging and automated thresholding approaches. Cyclic AMP signals were monitored using the H188 FRET-based reporter. Three-dimensional data were acquired using a Nikon A1R confocal microscope. Five slices from the apical to the basal side of the cell are shown. In the left column, FRET efficiency data, determined from linearly unmixed Turquoise and Venus images, is displayed. The middle column shows cAMP concentrations calculated from FRET efficiency, assuming the binding behavior is governed by the Hill equation with a Hill coefficient equal to 1. The right column displays localized regions of cAMP concentrations that were determined using a region-of-interest based software called S8. It is important to note that S8 data processing includes both spatial and temporal smoothing that is statistically guided by the software.

Treatment of the HASMC shown in Figure 3 with PGE₁ did not produce detectable apical to basal distributions of cAMP concentrations as treatment of the HASMC with isoproterenol did. After treatment, PGE₁ triggers higher concentrations of cAMP in the near-membrane regions of the cell shown in Figure 3. Cyclic AMP also appears to be produced at distinct locations within the cytoplasm at approximately the same level of the near-membrane region. These data demonstrate the potential of combining spectral FRET measurements with automated thresholding approaches in order to investigate the time course of localized subcellular signals.

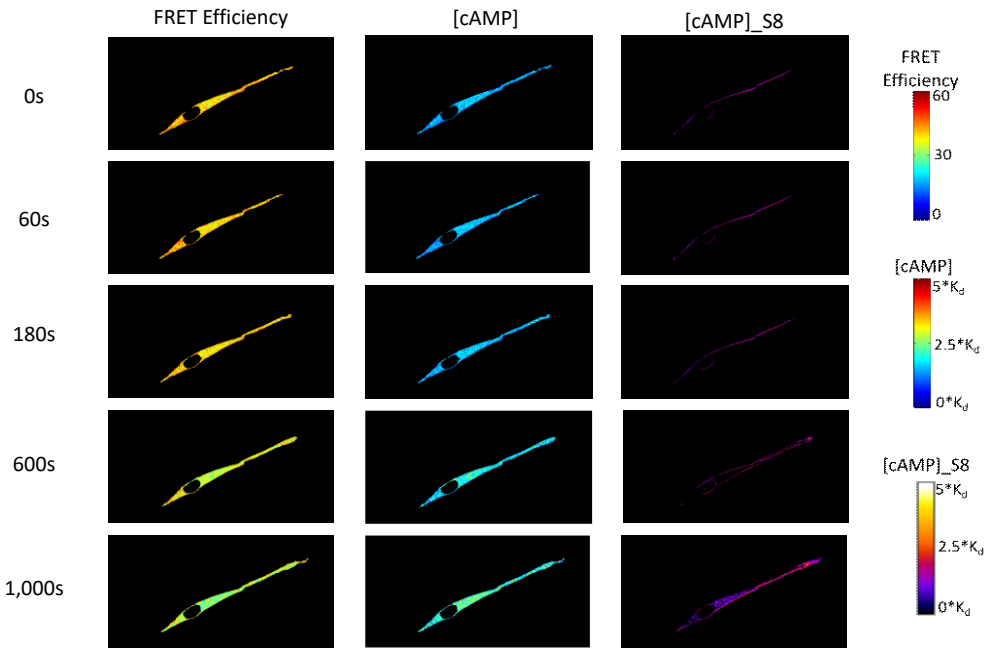


Figure 4: Visualization of time lapse PGE₁-induced cAMP signals in a HASMC using spectral imaging and automated thresholding approaches. Cyclic AMP signals were monitored using the H188 FRET-based reporter. The cell was treated at 60s with 0.1 μ M PGE₁. Three-dimensional data were acquired using a Nikon A1R confocal microscope. In the left column, FRET efficiency data, determined from linearly unmixing Turquoise and Venus images, is displayed. The middle column shows cAMP concentrations calculated from FRET efficiency, assuming the binding behavior is governed by the Hill equation with a Hill coefficient equal to 1. The right column displays localized regions of cAMP concentrations that were determined using a region-of-interest based software called S8. It is important to note that S8 data processing includes both spatial and temporal smoothing that is statistically guided by the software.

Near membrane regions were identified at all time points using the automated thresholding approaches implemented in S8 (Figure 4). At 600 seconds, S8 also identified intracellular regions of interest. Localized signals were observed in this image at 600 and 1000 seconds. These signals were only identified in later time point.

4. CONCLUSIONS AND FUTURE WORK

In this study, the use of an automatic region-of-interest based software for identifying localized regions of second messenger cAMP signals was demonstrated. This approach could be valuable for understanding the manner(s) that second messenger signals encode specific cell physiological events. Future goals of this research include quantifying and then understanding properties of localized second messenger signals, such as near-membrane localized cAMP.

ACKNOWLEDGEMENTS

This work was supported in part by funding through NIH grant numbers P01HL066299, R01HL058506, S10RR027535, NSF grant number 1725937, the University of Alabama at Birmingham Center for Clinical and Translational Science (CCTS), and the Economic Development Partnership of Alabama. Drs. Leavesley and Rich disclose financial interest in a start-up company, SpectraCyte LLC, founded to commercialize spectral imaging technologies.

REFERENCES

- [1] Amrani, Y., and Panettieri, R.A., "Airway smooth muscle: contraction and beyond," *The international journal of biochemistry & cell biology* 35(3), 272–276 (2003).
- [2] Prakash, Y., "Emerging concepts in smooth muscle contributions to airway structure and function: implications for health and disease," *American Journal of Physiology-Lung Cellular and Molecular Physiology* 311(6), L1113–L1140 (2016).

- [3] Sharma, P., Conaway, S., and Deshpande, D., “Bitter taste receptors in the airway cells functions” (2021).
- [4] Penn, R.B., and Benovic, J.L., “Regulation of heterotrimeric G protein signaling in airway smooth muscle,” Proceedings of the American Thoracic Society 5(1), 47–57 (2008).
- [5] Annamdevula, N.S., Sweat, R., Griswold, J.R., Trinh, K., Hoffman, C., West, S., Deal, J., Britain, A.L., Jalink, K., et al., “Spectral imaging of FRET-based sensors reveals sustained cAMP gradients in three spatial dimensions,” Cytometry Part A 93(10), 1029–1038 (2018).
- [6] Levy, S., Wilms, C.D., Brumer, E., Kahn, J., Pnueli, L., Arava, Y., Eilers, J., and Gitler, D., “SpRET: Highly sensitive and reliable spectral measurement of absolute FRET efficiency,” Microscopy and Microanalysis 17(2), 176–190 (2011).
- [7] Leavesley, S.J., Annamdevula, N.A., Geurts, A., Pleshinger, D., and Rich, T.C., “Assessing drug-cell and drug-tissue interactions through spectral FRET imaging,” presented at Visualizing and Quantifying Drug Distribution in Tissue V, 2021, 116240D.
- [8] Klarenbeek, J., Goedhart, J., van Batenburg, A., Groenewald, D., and Jalink, K., “Fourth-generation epac-based FRET sensors for cAMP feature exceptional brightness, photostability and dynamic range: characterization of dedicated sensors for FLIM, for ratiometry and with high affinity,” PloS one 10(4), e0122513 (2015).